Chapter

Airframe-Propulsion Integration Design and Optimization

Yao Zheng, Shuai Zhang, Tianlai Gu, Meijun Zhu, Lei Fu, Minghui Chen and Shuai Zhou

Abstract

Airframe-propulsion integration design is one of the key technologies of the hypersonic vehicle. With the development of hypersonic vehicle design method, CFD technology, and optimization method, it is possible to improve the conceptual design of airframe-propulsion integration both in accuracy and efficiency. In this chapter, design methods of waverider airframes and propulsion systems, including inlets, nozzles, isolators, and combustors, are reviewed and discussed in the light of CFD analyses. Thereafter, the Busemann inlet, a three-dimensional flow-stream traced nozzle, and a circular combustor together with a cone-derived waverider are chosen to demonstrate the airframe-propulsion integration design. The propulsion system is optimized according to the overall performance, and then the component such as the nozzle is optimized to obtain a better conceptual configuration.

Keywords: hypersonic vehicles, airframe-propulsion integration, conceptual design, optimization, computational fluid dynamics (CFD)

1. Introduction

Airframe-propulsion integration design is one of the key techniques of air-breathing hypersonic vehicles [1] to reduce overall drag and achieve positive thrust margins at hypersonic speeds [2]. The engine and airframe aerodynamics therefore become highly coupled [3]. Airframe-propulsion integration methodologies for the hypersonic vehicle have been extensively studied by many researchers [4–7]. A waverider is any supersonic or hypersonic lifting body that is characterized by an attached, or nearly attached, bow shock wave along its leading edge. Since its high lift-to-drag ratio, the waverider has become one of the most promising designs for air-breathing hypersonic vehicles. In the present study, the cone-derived waverider is used and optimized as the basis for the entire vehicle [8], and the engine is generated maintaining the shock wave attaching to the leading edge.

The design of the scramjet, which is a key part of the hypersonic vehicle technology, involves a lot of subjects. Typically, it includes components such as inlet, isolator, combustor, and nozzle. Considering both good performance of every component and interaction effects between each two components, the design progress becomes quite complicated. To effectively solve these difficulties, the present work proposes a method for integrated design and performance analysis of the scramjet flowpath. Aerodynamic performance and flow fields are analyzed one after another for the scramjet and component.

The whole process is in the order of zero-dimensional thermodynamic analysis [9], quasi-one-dimensional estimated analysis [10], and three-dimensional computational fluid dynamics analysis [11–13]. The scramjet flowpath is designed with an inward-turning inlet [12], a constant-area circular isolator, a circular combustor with a cavity [11], and a three-dimensional flow-stream traced nozzle [13]. Firstly, geometry parameters and flow conditions of both the inlet and the exit for each subsystem are obtained from the result of the stream function analysis and optimization [14]. Secondly, two design codes are developed, one of which is the quasi-one-dimensional estimation program for the combustor and the other is the aerodynamic force and heat estimation for the whole hypersonic vehicle. Lastly, the CFD method is applied for performance analysis of the jaws inlet, back pressure characteristics of the inlet with a constant-area isolator, and flow field characteristics of the combustor with a cavity.

2. Waveriders

In the waverider design, it is the first step to define the generation field and then the streamlines constituting the compression surface of the waverider. In the current study, the design conditions of the vehicle are chosen as follows: height of 25 km and free stream with the inflow Mach number to be 5.0. Thereafter, the shape together with the pressure distribution is determined. Typically, a waverider design process can be divided into: selection and design of the basic flow field in the flow direction, solving of the basic flow field, streamline tracing, and application of the osculating theory in the spanwise direction. After that, points representing streamlines are obtained. Streamlines and compression surface can be generated using CAD tools. For example, in this study, an automatic 3D configuration generation program based on the UG API is developed. Meanwhile, an aerodynamic force estimation program is built. Usually, remodel design of the waverider is needed for a specific purpose.

The basic flow field is usually a steady inviscid supersonic flow one, which is the core of the design of a waverider. Basic flow fields used for waverider design can be

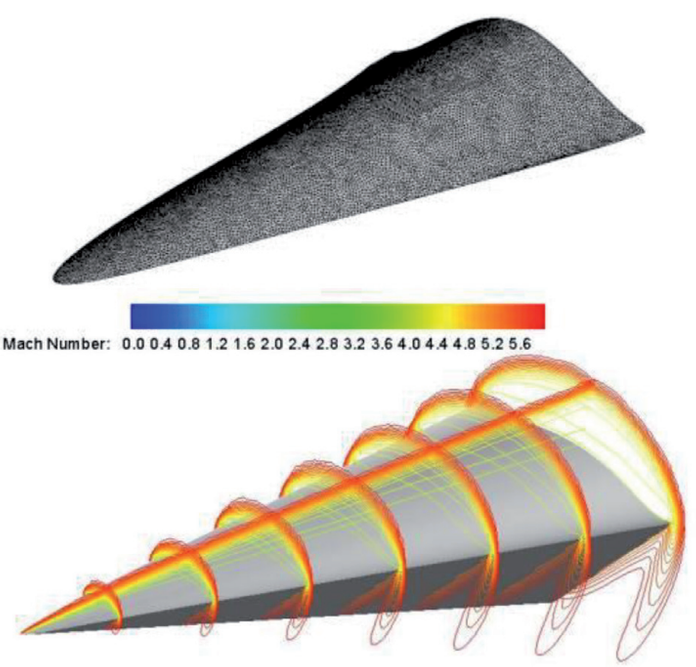

Figure 1.
Cone-derived waverider. (upper) Configuration with surface mesh for rapid estimation. (bottom) CFD simulation under design conditions.

classified into two types: steady two-dimensional (2D) planar or asymmetrical supersonic flow fields and three-dimensional (3D) supersonic flow fields. Since 2D planar or asymmetrical flow fields can be calculated easily by fast calculation methods such as the method of characteristics (MOC), most of the basic flow fields used for rapid design and optimization of waveriders are of the 2D planar or asymmetrical type.

The supersonic flow around a cone at a zero angle of attack, which is known as a conical flow field, is a typical 2D asymmetrical basic flow field. In 1968, Jones et al. [15] first used this kind of flow field to design a waverider known as the cone-derived waverider. The conical flow field is by far the most widely used basic flow field for waveriders, and the cone-derived waverider has become the most widely used waverider owing to the ease of its calculation and better volumetric efficiency than wedge-derived waverider on account of the concave streamlines being closer to the shock wave. **Figure 1** shows our designed cone-derived waverider configuration and numerical simulation results. The surrogate modes for aerodynamic shape optimization were carried out based on the values of lift-to-drag ratio and volumetric efficiency response [8]. In the present study, the commercial software Fluent and Insight are chosen for the numerical simulation and optimization, respectively.

3. Scramjet

Regarding the conceptual design of scramjet, the stream thrust analysis [9] was superior to that of the thermodynamic cycle or first law analyses as it managed to account for several phenomena such as the geometry of the combustor, the velocity, mass of the fuel, and the exhaust outlet pressure not matching the ambient. **Figure 2** briefly introduces the design procedure and method of scramjet.

A scramjet was first designed by using stream thrust analysis, to obtain the overall parameters and flow state parameters at the in-/outlet of each components. When the stream thrust was analyzed, a group of state parameters were determined such as pressure, density, and temperature together with velocity and areas in each component's inlet and outlet. These parameters were delivered to the following two-dimensional components' design of the inlet, isolator, combustor, and nozzle. When the overall dimension of the scramjet internal flow passage was determined, the performance of a scramjet that allowed a supersonic flow to pass through the engine without choking in the inlet throat, combustor, and nozzle were analyzed by the quasi-one-dimensional evaluation program.

Using the above conceptual design method and performance evaluation, the initial design and analysis of a scramjet were performed. The optimization was conducted to generate more practical results based on the specific objectives. The flow chart describing the conceptual design method and optimization process is shown in **Figure 3**. As the design and evaluation of scramjet are highly nonlinear problems,

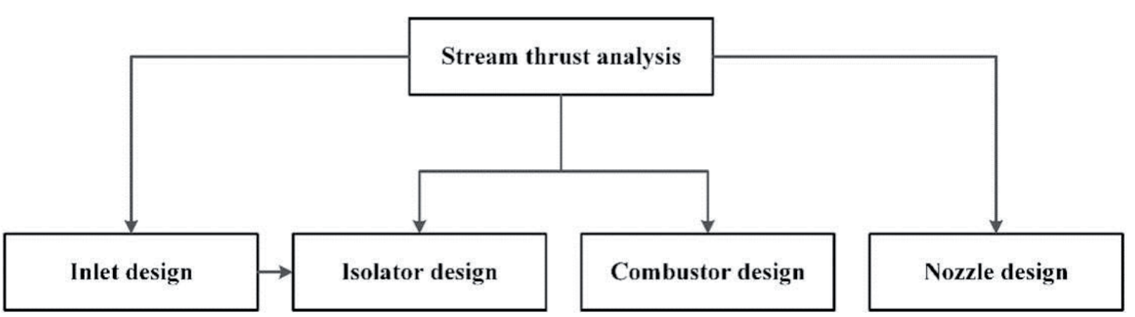

Figure 2.
Flow chart of conceptual scramjet design.

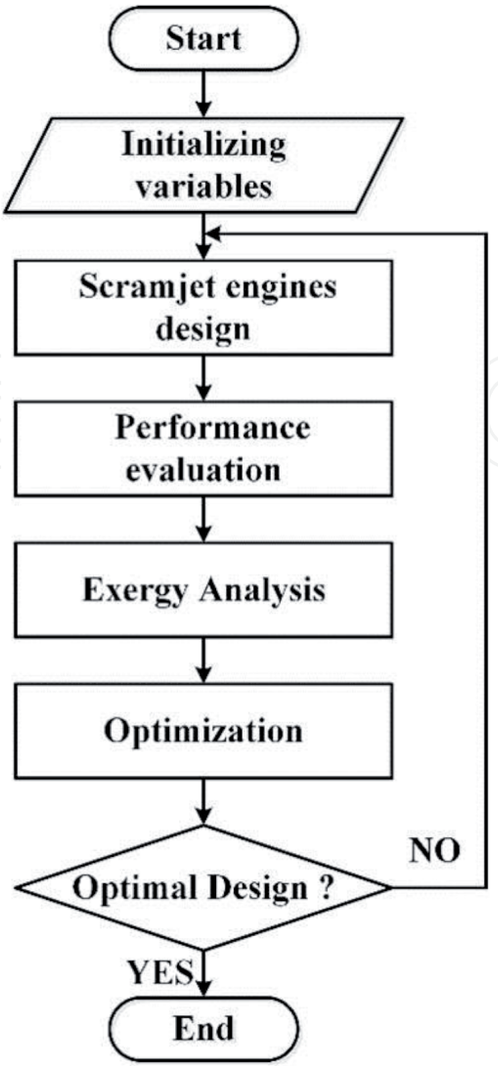

Figure 3.
Flow chart of the conceptual design and optimization process.

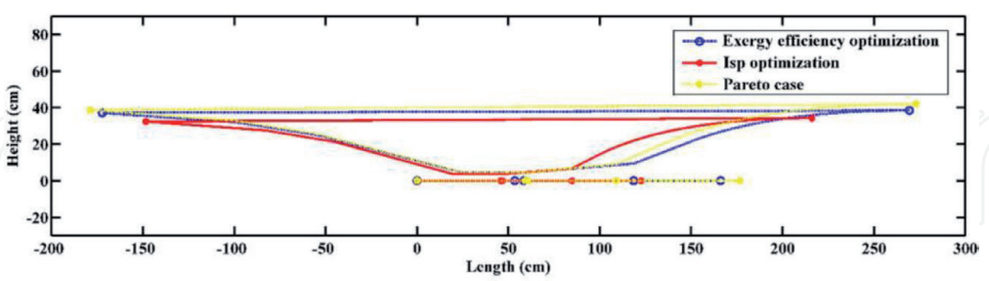

Figure 4.
Comparison of three optimal vehicle geometry shapes.

a multi-island genetic algorithm was chosen as the single-objective optimization algorithm, and a nondominated sorting genetic algorithm was selected as the multi-objective optimization algorithm. After the scramjet was designed and evaluated, the optimization was conducted to study how exergy works in the complex integrated system and to find which design variables play relatively important roles in this evaluation system. **Figure 4** shows the vehicle geometry shapes of different optimization objective cases. Three-dimensional design result of the scramjet can be seen in **Figure 5**. The detailed design methods for each part will be introduced in the following.

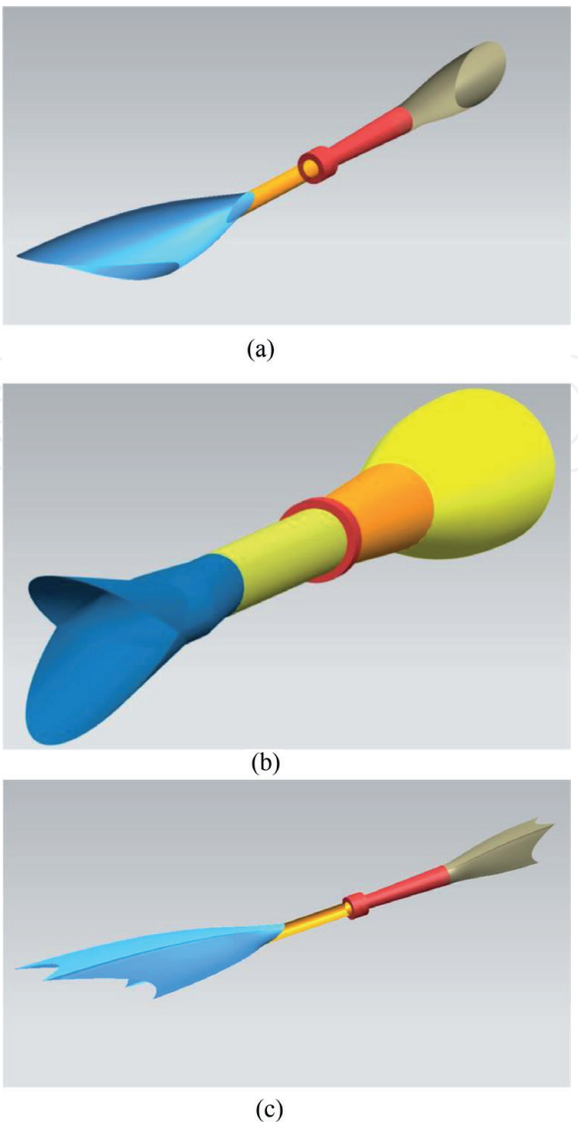

Figure 5.
Conceptual three-dimensional scramjet design: (a) Busemann inlet, circular isolator and combustor, three-dimensional asymmetric nozzle. (b) Jaws inlet, circular isolator and combustor, three-dimensional symmetric nozzle. (c) REST inlet, circular isolator and combustor, three-dimensional asymmetric circle-to-rectangle nozzle.

3.1 Inlets

Various prototypes of hypersonic inlet have been proposed since the 1960s. Kothari introduced the radial deviation parameter and categorized the inlets as inward-turning inlets, outward-turning inlets, and two-dimensional inlets [16]. Unlike the other two groups, inward-turning inlets exhibit accumulation of flows in the central part. The advantages of inward-turning designs, especially those approaching a completely round combustor entrance shape, are several fold. From structural and wetted area perspectives, a more round design provides better performance than a rectangular or two-dimensional configuration. Lower wetted surface area in the combustor for an equivalent level of thrust of course means lower heating loads and lower drag. Moreover, corner flows need be much less of a concern with inward-turning geometries. Low aspect ratios at the isolator, which are characteristic of inward-turning inlets, also result in operational advantages. In **Figure 6**, typical inward-turning inlets such as Busemann, REST, and Jaws inlets were designed and built using CAD tools.

The performance of designed inlets under on and off design conditions was numerically investigated [12]. **Figure 7** shows the comparison on the performance

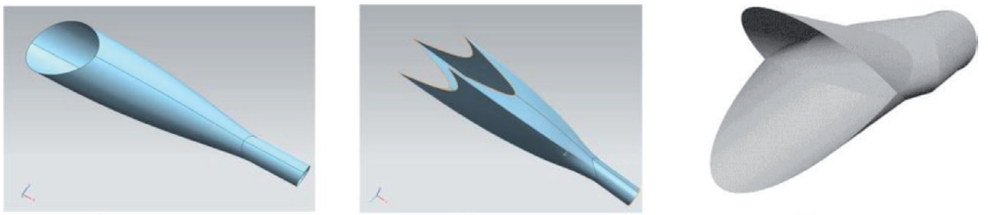

Figure 6.
Several inward-turning inlets design. (a) Busemann. (b) REST. (c) Jaw's.

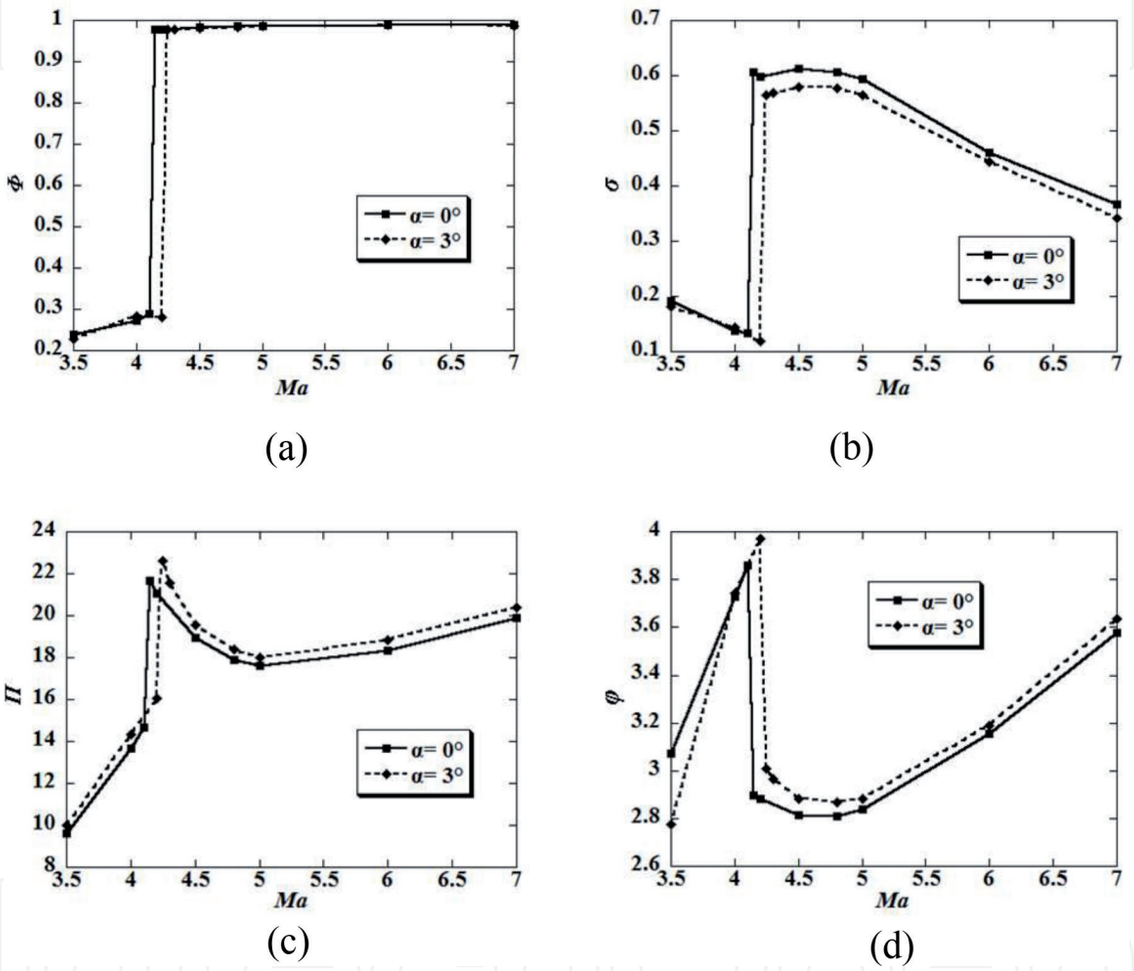

Figure 7.
Performance parameters of Jaws inlet under different inflow Ma: (a) mass capture ratio, (b) total pressure recovery coefficient, and (c) static pressure ratio (d) temperature ratio.

of one Jaws inlet under different inflow Mach numbers and two different angles of attack. In **Figure 8**, numerical simulations were carried out for Jaws inlet under different back pressures. In addition, performances of different inward-turning inlets were also compared using numerical simulations.

3.2 Isolators

An isolator is necessary in scramjet to prevent inlet to unstart under high back pressure due to heat release in the combustor. The backpressure can cause the isolator flow to fluctuate violently. As the back pressure exceeds the critical value, the inlet can unstart, which causes the flow field to become unstable and oscillate unsteadily, with the drag increasing sharply and causing the engine to lose thrust.

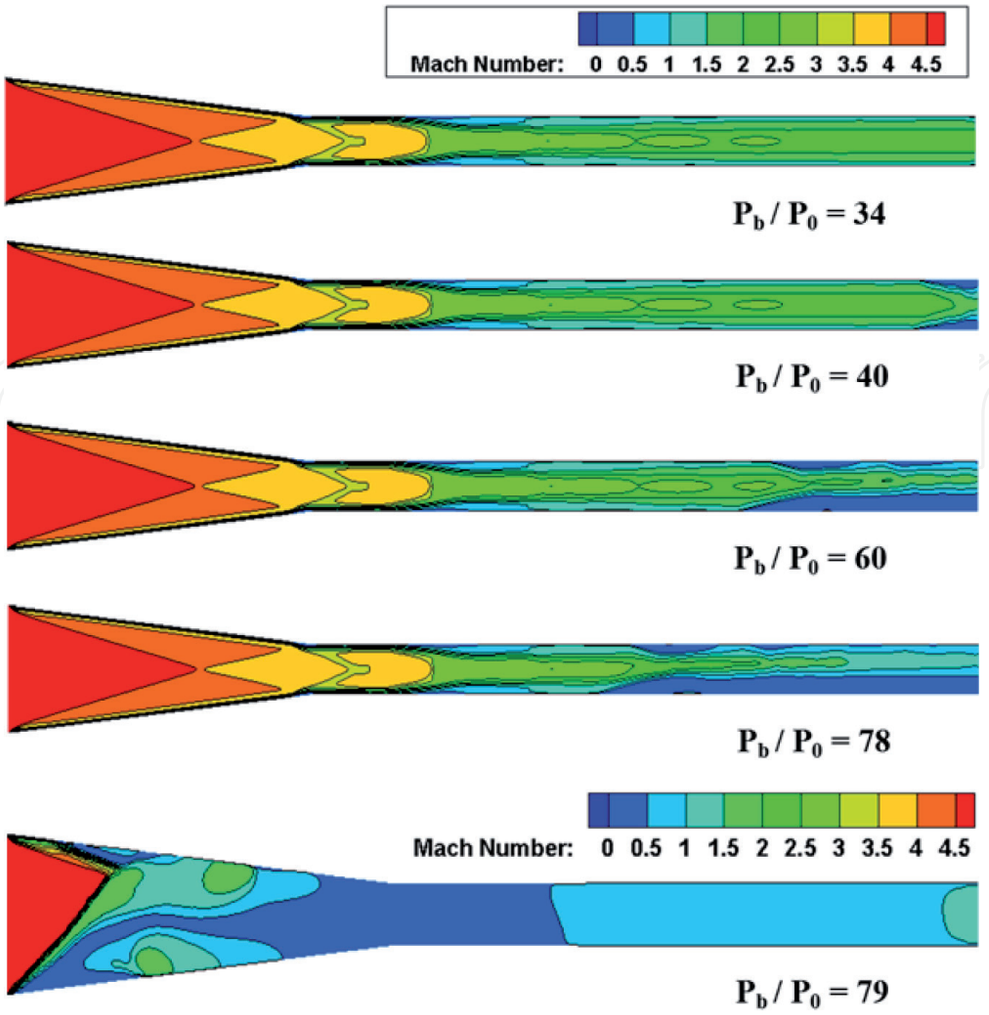

Figure 8.
Mach number contours of Jaws inlet flow fields under different back pressures.

In the isolator, due to the close coupling of the boundary layer and the supersonic core flow through shock waves and expansion waves, the flow structure of a shock train is rather complex even at very simple incoming flow conditions and wall conditions. Correspondingly, it is important to understand the mechanism of the pseudo-shock motion in the isolator. **Figures 9** and **10** show the comparison between numerical simulation results and experimental observation to understand the complex pseudoshock train in the circular and rectangular isolators, respectively. The conceptual design of isolator with a given shape of the inlet is conducted by using the empirical length formula [14]. Meanwhile, the isolator is further truncated with the passive wedge flow control. **Figure 11** shows the simulation results of design without and with the wedge flow control, as shown in the left and right of the figure.

3.3 Combustors

In the combustor, injection fuels mix with incoming air and burn to release large amounts of energy. In the conceptual design, the combustor length includes the ignition length and the combustion length. The ignition length can be obtained by multiplying the ignition delay time which referred to Balakrishnan and Williams [17] by the relative velocity between air and fuel. The combustion length can be modeled based on the study of Hasselbrink [18] and Smith [19]. **Figure 12** shows the conceptual design result of the combustor.

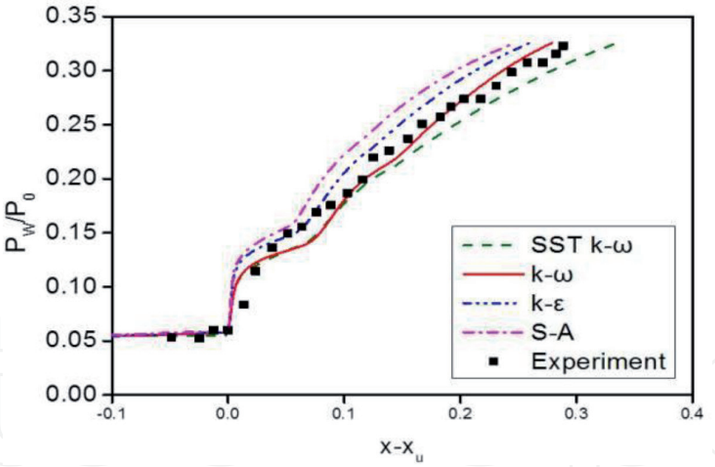

Figure 9.
Pressure distribution along wall using different turbulent models.

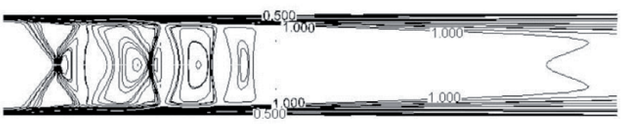

Figure 10.
Contour of Mach number in the central symmetry plane.

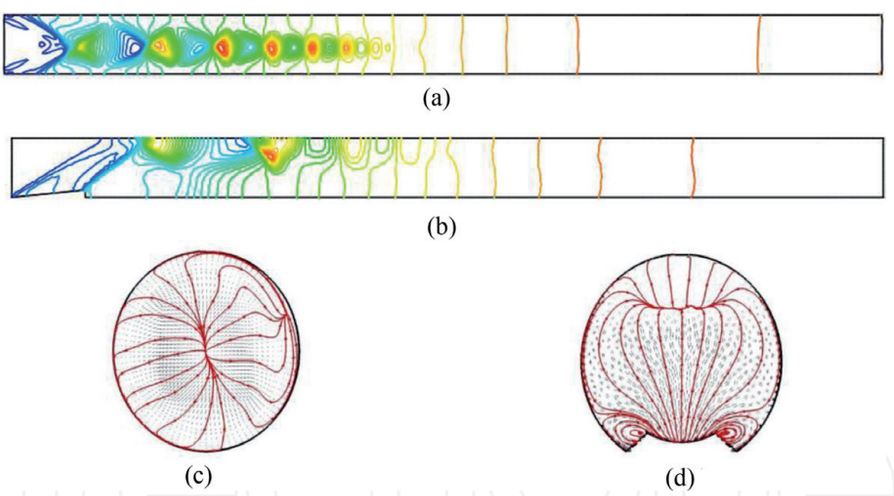

Figure 11.
Simulation result of circular isolator. (a) Pressure contour of baseline design. (b) Pressure contour of baseline design with wedge control. (c) Velocity distribution of baseline design at x = 300 mm. (d) Velocity distribution of baseline design with wedge control at x = 300 mm.

According to the combustion in scramjet engines, the time available for fuel injection, mixing, and combustion is very short. It is important to study the flame holding mechanisms. The presence of normal fuel injector inside the combustor generates a detached normal shock toward the upstream direction of the injector. As a result, there is a formation of separation region which may influence the efficiency of the combustor. As shown in **Figure 13**, numerical simulations were performed to understand the related flow structures. Another alternative method for better-mixing phenomena in scramjet combustor is to use cavity flame holders. Numerical studies on the cavity in the combustor were carried out, as can be seen in **Figure 14**. The fuel injection position was numerically investigated to find out an appropriate value, as shown in **Figure 15**.

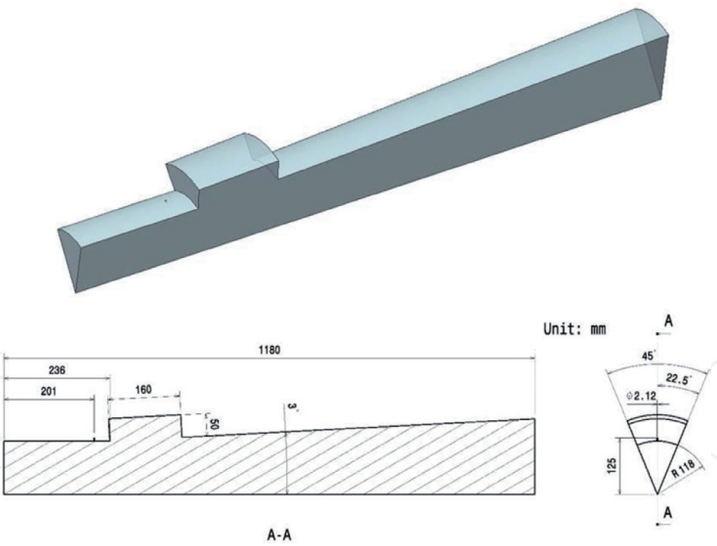

Figure 12.
Geometry of combustor with cavity in 1/8 size.

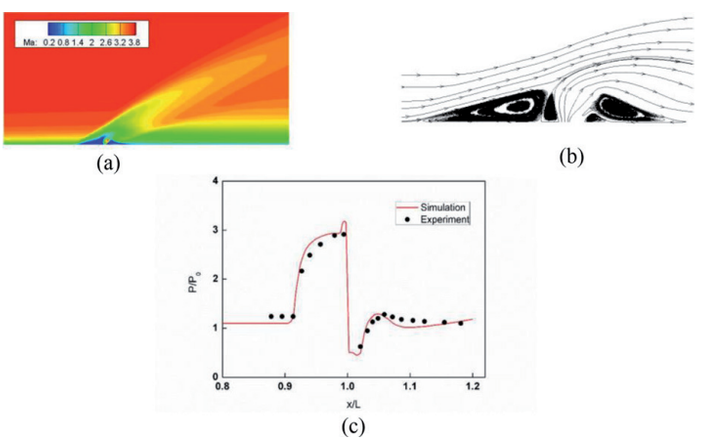

Figure 13.
Simulation of normal inlet under supersonic inflow: (a) Mach contour, (b) streamline, and (c) pressure distribution along wall.

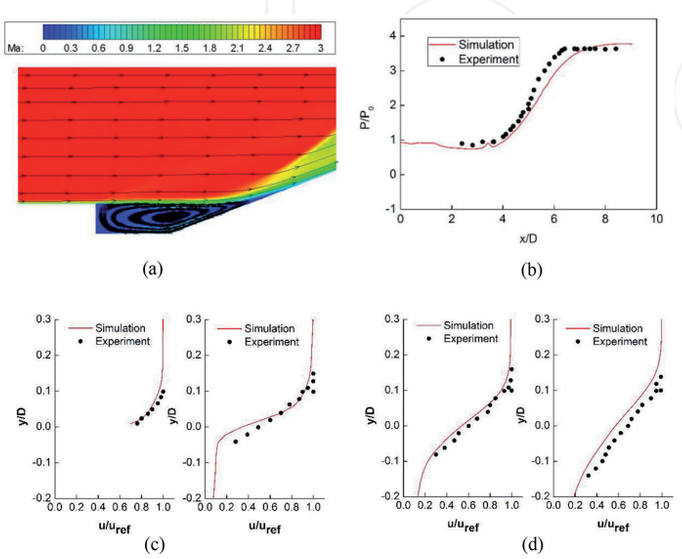

Figure 14.
Numerical simulation results of cavity under supersonic inflow. (a) Ma contour and streamline. (b) Pressure distribution along the cavity wall. (c) Velocity distribution across the shear layer at x = 25.4 and 38.1 mm. (d) Velocity distribution across the shear layer at x = 63.5 and 88.9 mm.

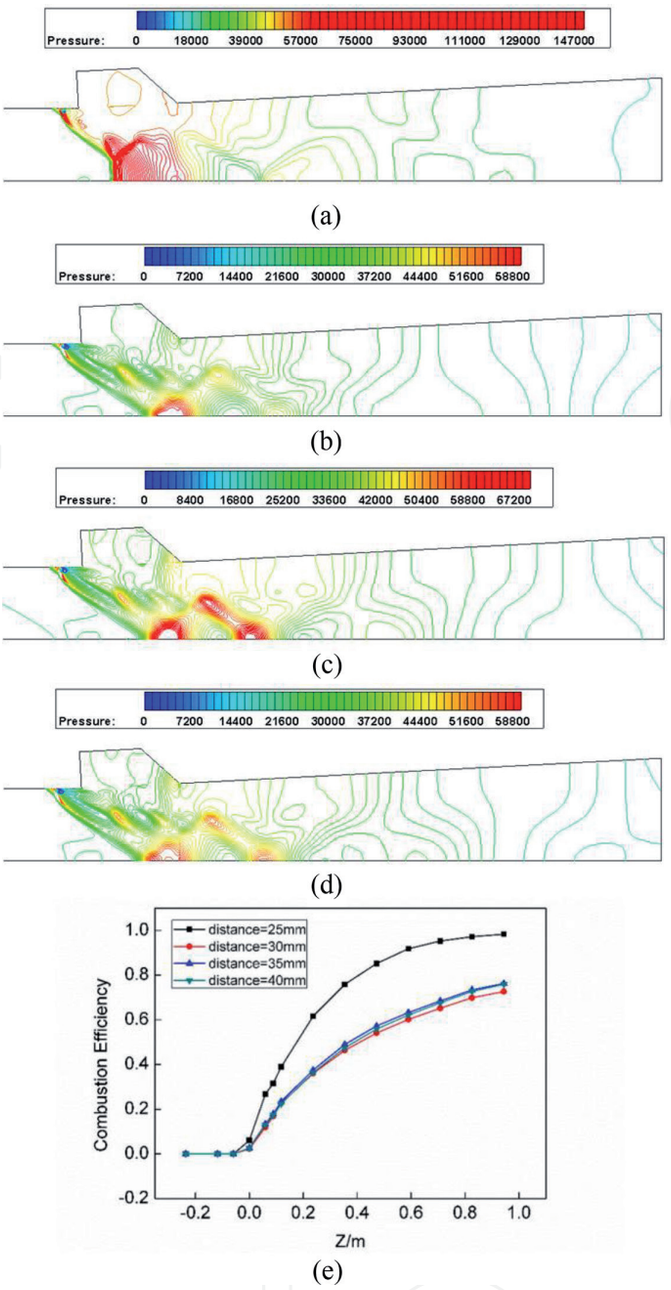

Figure 15.
Pressure contour (unit of P_a) and combustion efficiency for four fuel injection positions. (a) Distance between injection nozzle and cavity leading edge of 25 mm. (b) Distance between injection nozzle and cavity leading edge of 30 mm. (c) Distance between injection nozzle and cavity leading edge of 35 mm. (d) Distance between injection nozzle and cavity leading edge of 40 mm. (e) Comparison on the combustion efficiency.

The cavity has a great influence on the performance of supersonic combustors, such as combustion efficiency, drag characteristics, and flame stability. The impact of the cavity parameter variation on the performance of combustors is complex coupled. A surrogate model-based optimization and parameter analysis of the cavities in three-dimensional supersonic combustors with transverse fuel injection upstream were performed. The length, depth, and sweepback angle of cavities were first designed by orthogonal experiment. Numerical simulations were applied to analyze the performance and flow fields of the test cases. Surrogate models of the combustion efficiency and total pressure recovery coefficient with the design variables were constructed.

Based on the complex system optimization strategy, optimization of the cavity parameters was carried out twice to provide the Pareto front by the non-dominated

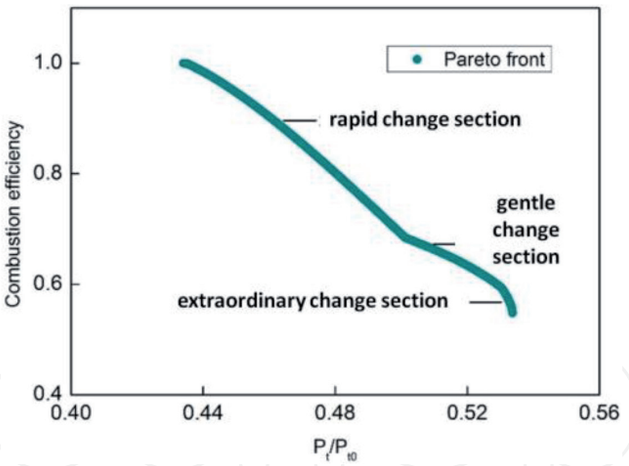

Figure 16.
Pareto front of the cavity optimization.

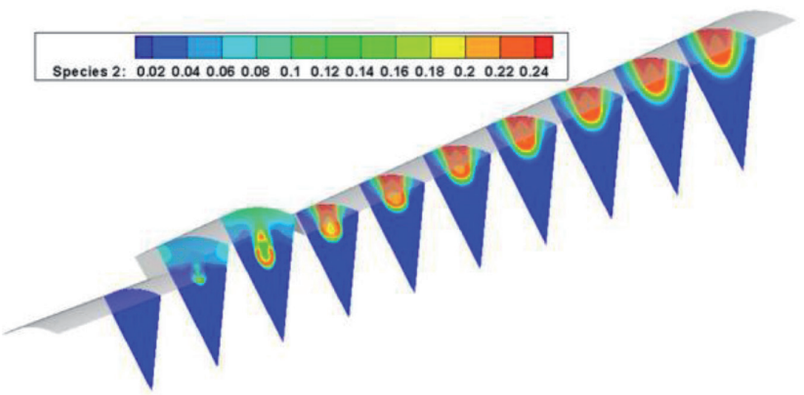

Figure 17.
Contour of the mass fraction of H_2O at different cross sections.

sorting genetic algorithm (NSGA-II). The results show that the optimal cavity configurations can be divided into narrow deep type, as can be seen in **Figure 16**, shallow long type, and medium deep and long type, which correspond to rapid change section, gentle change section, and extraordinary change section in the Pareto front. The combustion efficiency has a negative correlation with the length of cavities and a positive correlation with the depth of cavities, whereas the total pressure recovery coefficient has the opposite situations. Both combustion efficiency and total pressure recovery coefficient have few positive correlations with the sweepback angle. The combustors in the gentle change section have more uniform pressure distribution and higher total pressure recovery coefficient, which should be preferred when there is no need of high combustion efficiency. Optimized combustor configurations were simulated and verified compared to the baseline design, as shown in **Figure 17**.

3.4 Nozzles

A supersonic nozzle design is a significant work for hypersonic vehicles, which devotes to produce most of the thrust force and helps to improve the vehicle's internal/external integral level. Two-dimensional (2D) and axisymmetric minimum length nozzles (MLNs) with constant and variable specific heat were designed using the method of characteristics (MOCs) [20, 21], as can be seen in

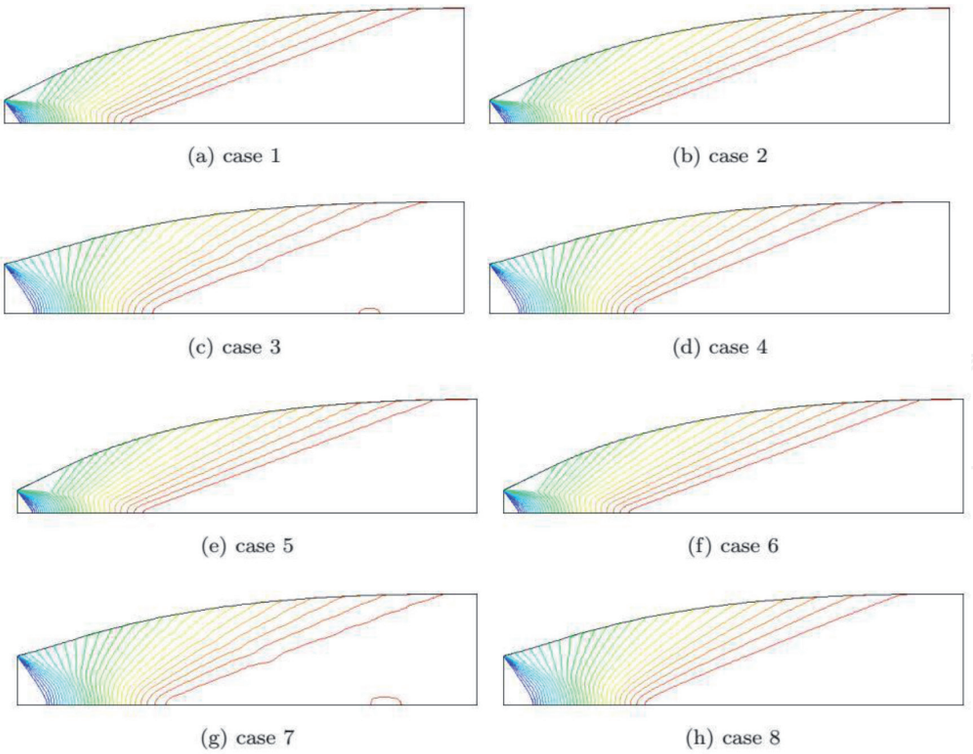

Figure 18.
Isograms of flow field Mach number in different nozzles.

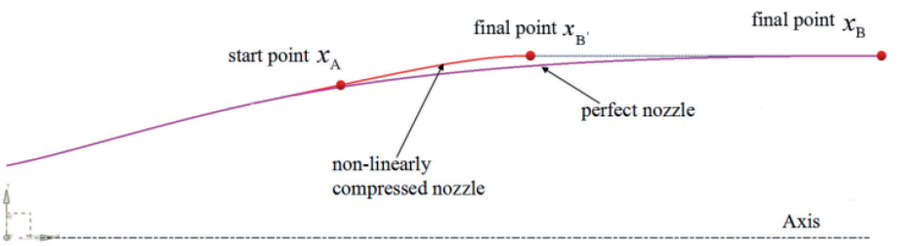

Figure 19.
Diagram of nonlinearly compressed nozzle process.

Figure 18, where Case 1 is for constant specific heat, 2-D and conservation of mass; Case 2 for constant specific heat, 2-D and eliminating wave theory; Case 3 for constant specific heat, axisymmetrical and conservation of mass; Case 4 for constant specific heat, axisymmetrical and eliminating wave theory; Case 5 for varying specific heat, 2-D and conservation of mass; Case 6 for varying specific heat, 2-D and eliminating wave theory; Case 7 for varying specific heat, axisymmetrical and conservation of mass; and finally, Case 8 for varying specific heat, axisymmetrical and eliminating wave theory. MOC is a numerical technique which has great advantages in accuracy and efficiency for solving hyperbolic partial differential equations.

After the two-dimensional supersonic nozzle design is finished, the flow field is simultaneously obtained with the MOC solution. Concerning the three-dimensional nozzle design, using the streamline tracing technique, the present work designed a three-dimensional asymmetric nozzle with a pre-determined offset circular entrance. However, the nozzles designed by MOC may have excellent thrust performance, but the length goes beyond the geometry constraints of the scramjet engine and does not meet the trim and lift-to-drag ratio requirements. As shown in **Figure 19**, a nonlinear compression technique can be used to truncate the streamline of the perfect nozzle, by preserving the initial major expansion parts of nozzle

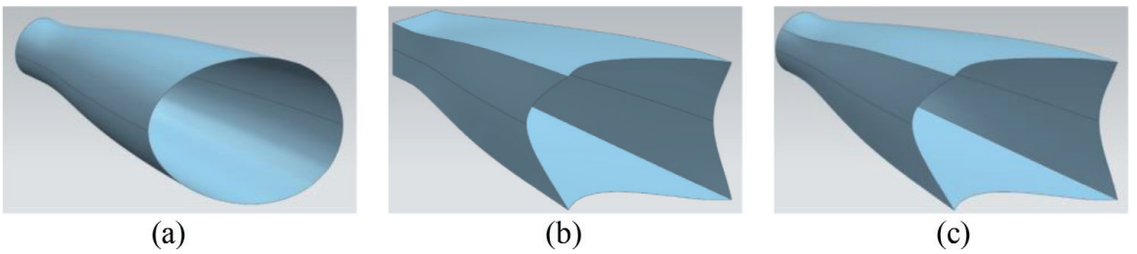

Figure 20.
Three-dimensional nonlinear truncated streamline traced nozzle: (a) circular, (b) rectangle, and (c) circular to rectangle.

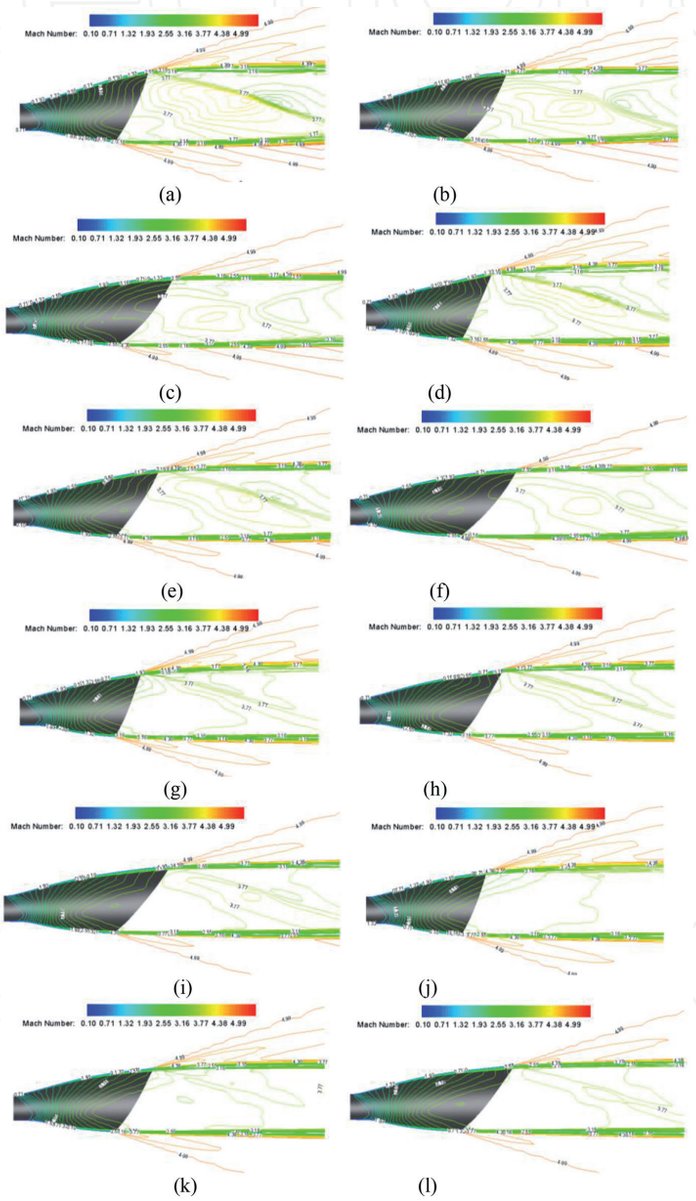

Figure 21.
Contour of Mach number under different truncation parameters. (a) 0.10–0.50 (b) 0.10–0.60 (c) 0.10–0.70 (d) 0.20–0.50 (e) 0.20–0.60 (f) 0.20–0.70 (g) 0.30–0.50 (h) 0.30–0.60 (i) 0.30–0.70 (j) 0.40–0.50 (k) 0.40–0.60 (l) 0.40–0.70 (First parameter is A = *x* B′/*x* B *and second one is* B = *x* A/*x* B*).*

and making the remaining nonlinear compressed. **Figure 20** shows three kinds of typical generated three-dimensional asymmetric nozzle. Numerical studies were performed to investigate the design parameters, such as the pre-determined offset size, the nonlinear truncation parameters, and so on. **Figure 21** shows the simulated Mach number contours with different truncation parameters.

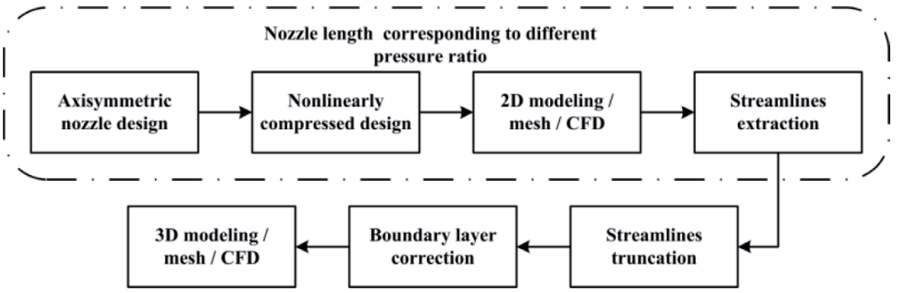

Figure 22.
Three-dimensional asymmetric nozzle design process.

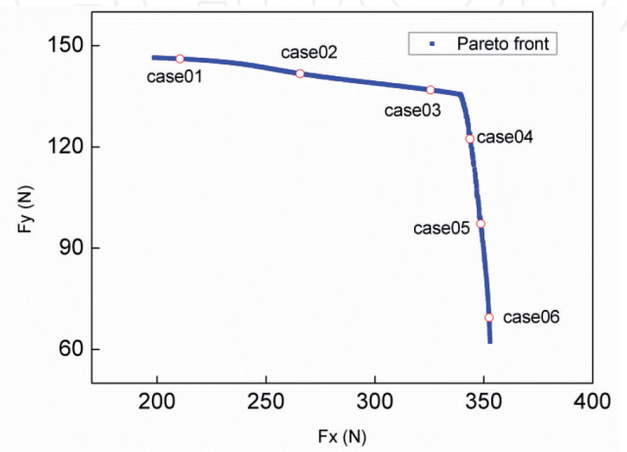

Figure 23.
Pareto front with six selected cases.

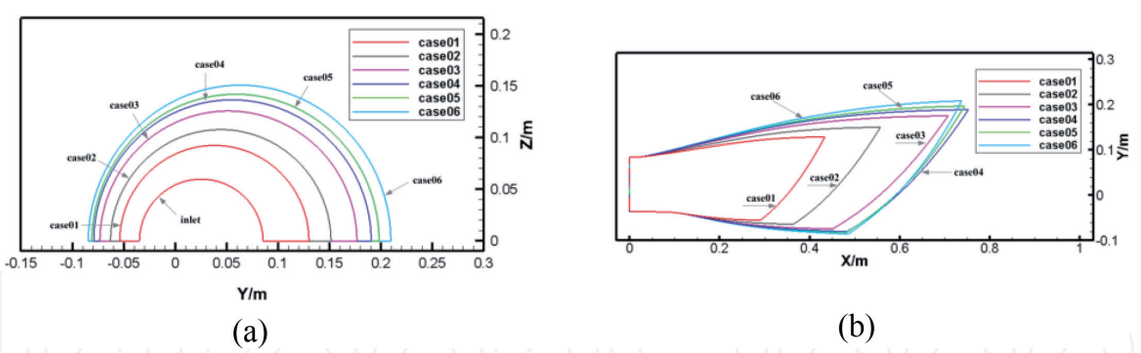

Figure 24.
Inlet and outlet shapes of six selected optimization: (a) inlet shape and (b) outlet shape.

Figure 22 shows the whole design process. Thereafter, a multiobjective design optimization has been performed, using orthogonal design, Kriging surrogate model with objective functions of thrust and lift force. Numerical simulations were conducted to validate the accuracy of surrogate models and to provide details of flow fields. The optimization results were examined to investigate the key factors and underlying flow physics that influenced the nozzle performance and to offer a preliminary guide to design a better nozzle with a suitable length. Six cases were selected from the Pareto front as illustrated in **Figures 23** and **24**. The design variables of these cases are used to obtain new design results. New numerical simulations were performed to verify the reliability of surrogate models and to provide a deeper insight of nozzle performance, as can be seen in **Figure 25**.

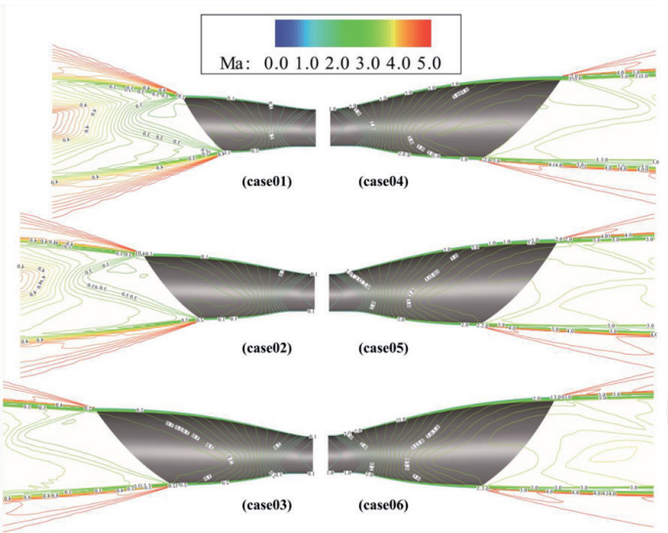

Figure 25.
Mach number contour of six Pareto front cases.

4. Airframe-propulsion integration

The integration method for the cone-derived waverider and scramjet is introduced as the following. The basic Busemann flow field is decided according to the area ratio between inlet and outlet surfaces of the inward-turning inlet, which can be calculated using the stream thrust analysis. As a result, the Busemann inlet can be obtained. The length of the Busemann inlet is too large, and its upper surface of inlet is horizontal which is not appropriate for integration with the waverider. The Busemann inlet is then truncated.

The angle of the truncation cone should not be too large and is chosen between 3 degree and 5 degree in the present studies. Meanwhile, the semiapex angle of the truncation cone should be smaller than that of the waverider. Accordingly, iterations are necessary to find out the appropriate basic Busemann flow field. The basic flow field of the cone-derived waverider is decided with the design parameters, for example, the inflow Mach number and an appropriate compression angle. The shock angle and the semiapex angle can be calculated. As mentioned before, the semiapex angle must be larger than that of the truncated Busemann inlet. **Figure 26** shows the integration of the inlet and the waverider compression surface. An integration example of the cone-derived waverider and the scramjet can be seen in **Figure 27**.

Figure 28 compares the contour of Mach number of original cone-derived waverider and integrated vehicle. It can be observed that shock waves attach the bottom leading edges of surfaces of both vehicles. **Figure 29** shows simulation

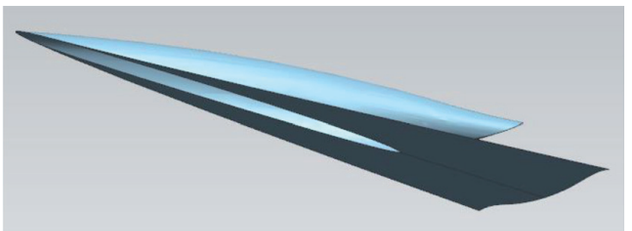

Figure 26.
Integration of cone-derived waverider and truncated Busemann inlet.

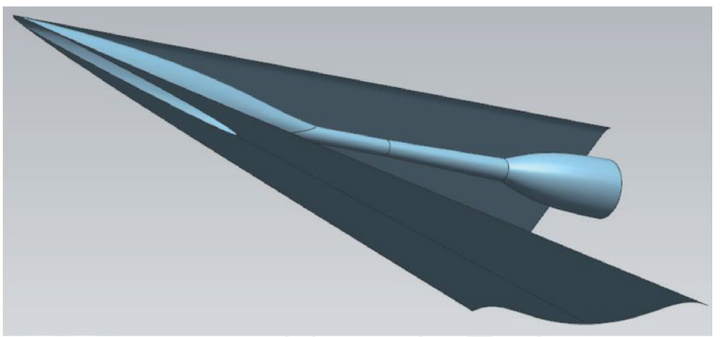

Figure 27.
Integration vehicle.

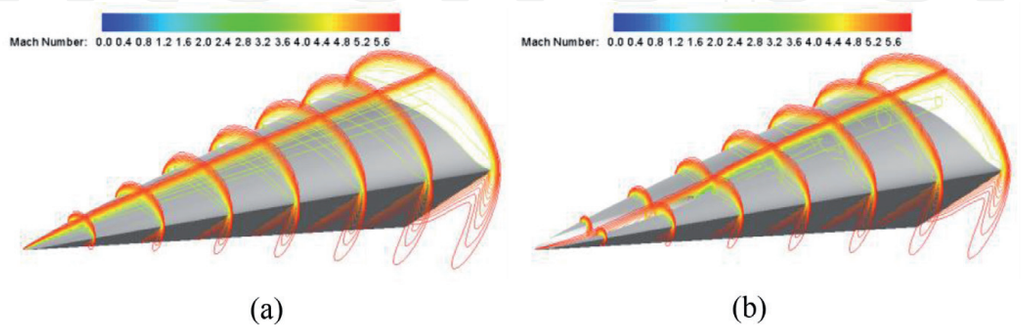

Figure 28.
Comparison on simulated Mach contour of original waverider and integration vehicle. (a) Original waverider. (b) Integration vehicle.

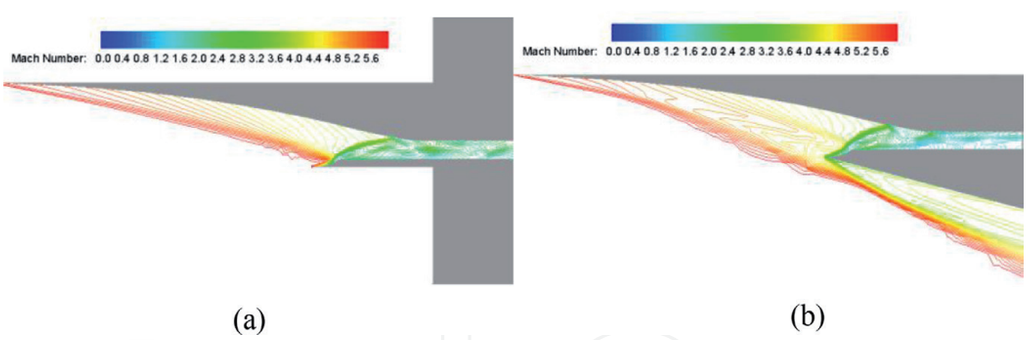

Figure 29.
Comparison on simulated Mach contour of original Busemann inlet and integration vehicle. (a) Original Busemann inlet. (b) Integration vehicle.

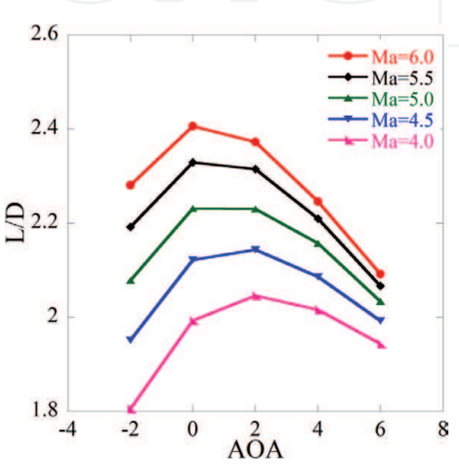

Figure 30.
Lift-to-drag ratio versus angle of attack of the integration vehicle.

results of the original truncated Busemann inlet and the integrated vehicle. There is a small difference between them since the integration would change the inflow for the inlet. However, the difference is not large. **Figure 30** shows the lift-to-drag ratio versus angle of attack of the integration vehicle.

5. Conclusions

Airframe-propulsion integration design method is investigated in the present study. The design methods for the waverider and each components of the scramjet are introduced. The integration method between the waverider and the scramjet is described. The overall optimization for the whole scramjet flowpath is optimized with quick engineering estimation method to provide appropriate performance criteria, which are then used to design three-dimensional component configurations.

Additionally, optimization is performed for the waverider and scramjet components with surrogate modes and CFD simulations. Numerical studies are carried out to find out the performances of the waverider and each component of the scramjet to check whether they can work normally under the design conditions. In the future, the design method for the dual-mode combustor (ramjet and scramjet) will be considered. The numerical simulation for the whole scramjet or dual-mode combustor is necessary to perform to verify the design method.

Conflict of interest

The authors declare that there is no conflict of interest regarding the publication of this work.

Author details

Yao Zheng*, Shuai Zhang, Tianlai Gu, Meijun Zhu, Lei Fu, Minghui Chen and Shuai Zhou
Center for Engineering and Scientific Computation, and School of Aeronautics and Astronautics, Zhejiang University, Hangzhou, Zhejiang, China

*Address all correspondence to: yao.zheng@zju.edu.cn

References

[1] Huang W, Wang ZG. Numerical study of attack angle characteristics for integrated hypersonic vehicle. Applied Mathematics and Mechanics. 2009;**30**(6):779-786. DOI: 10.1007/s10483-009-0612-y

[2] O'Neill MK, Lewis MJ. Optimized scramjet integration on a waverider. Journal of Aircraft. 1992;**29**(6):1114-1121. DOI: 10.2514/3.56866

[3] Huang W, Wang ZG, Jin L, Liu J. Effect of cavity location on combustion flow field of integrated hypersonic vehicle in near space. Journal of Vision. 2011;**14**(4):339-351. DOI: 10.1007/s12650-011-0100-3

[4] Stevens DR. Practical Considerations in Waverider Applications. AIAA Paper 92-42471992. DOI: 10.2514/6.1992-4247

[5] Takashima N, Lewis MJ. Waverider Configurations Based on Nonaxisymmetric Flow Fields for Engine-Airframe Integration. AIAA Paper 94-03801994. DOI: 10.2514/6.1994-380

[6] Takashima N, Lewis MJ. Engine-Airframe Integration on Osculating Cone Waverider-Based Vehicle Designs. AIAA Paper 96-25511996. DOI: 10.2514/6.1996-2551

[7] O'Brien TF, Lewis MJ. Rocket-based combined-cycle engine integration on an osculating cone waverider vehicle. Journal of Aircraft. 2001;**38**(6):1117-1123. DOI: 10.2514/2.2880

[8] Ji T, Wang Y, Zhang J, Zhang S. Surrogate models characteristic analysis and optimization for waverider aerodynamic design (in Chinese). Journal of Solid Rocket Technology. 2015;**38**(4):451-457. DOI: 107673/j.issn.1006-2793.2015.04.001

[9] William H, Pratt H, David T. Hypersonic Airbreathing Propulsion. 5th ed. Washington, DC: American Institute of Aeronautics and Astronautics Inc; 1994. 173 p

[10] Birzer CH, Doolan CJ. Quasi-one-dimensional model of hydrogen-fueled scramjet combustors. Journal of Propulsion and Power. 2009;**25**(6):1220-1225. DOI: 10.2514/1.43716

[11] Zhu M, Gu T, Zhang S, Zheng Y. Optimization and parameter analysis of cavity in a three-dimensional supersonic combustor (in Chinese). Journal of Propulsion Technology. 2018;**39**(8):1780-1789. DOI: 10.13675/j.cnki.tjjs.2018.08.012

[12] Gu T, Zhang S, Zheng Y. Performance of a jaws inlet under off-design conditions. Proceedings of the Institution of Mechanical Engineers, Part G: Journal of Aerospace Engineering. 2017;**231**(2):294-305. DOI: 10.1177/0954410016636163

[13] Zhu M, Fu L, Zhang S, Zheng Y. Design and optimization of three-dimensional supersonic asymmetric truncated nozzle. Proceedings of the Institution of Mechanical Engineers, Part G: Journal of Aerospace Engineering. 2018;**232**(15):2923-2935. DOI: 10.1177/0954410017718567

[14] Zhu M, Zhang S, Zheng Y. Conceptual design and optimization of scramjet engines using the exergy method. Journal of the Brazilian Society of Mechanical Sciences and Engineering. 2018;**40**(12):553. DOI: 10.1007/s40430-018-1468-y

[15] Jones JG, Moore KC, Pike J, Roe PL. A method for designing lifting configurations for high supersonic speeds, using axisymmetric flow fields. Ingenieur Archiv. 1968;**37**:56-72. DOI: 10.1007/BF00532683

[16] Kothari AP, Tarpley C, McLaughlin TA, et al. Hypersonic vehicle design using

inward turning flowfields. In: 32nd Joint Propulsion Conference and Exhibit, 1996-2552. 1996

[17] Balakrishnan G, Williams F. Turbulent combustion regimes for hypersonic propulsion employing hydrogen-air diffusion flames. Journal of Propulsion and Power. 1994;**10**(3):434-437. DOI: 10.2514/3.23754

[18] Smith S, Mungal M. Mixing, structure and scaling of the jet in crossflow. Journal of Fluid Mechanics. 1998;**357**:83-122. DOI: 10.1017/S0022112097007891

[19] Hasselbrink EF, Mungal M. Transverse jets and jet flames. Part 1. Scaling laws for strong transverse jets. Journal of Fluid Mechanics. 2001;**443**: 1-25. DOI: 10.1017/S0022112001005146

[20] Fu L, Zhang S, Zheng Y. Performances analysis of asymmetric minimum length nozzles. International Journal of Modeling, Simulation, and Scientific Computing. 2016;**7**(2):1-12. DOI: 10.1142/S1793962316500215

[21] Lei F, Zhang S, Zheng Y. Design and verification of minimum length nozzles with specific/variable heat ratio based on method of characteristics. International Journal of Computational Methods. 2016;**13**(6):1-13. DOI: 10.1142/S0219876216500341